



**HAL**  
open science

# LUMPED-PARAMETERS EQUIVALENT CIRCUIT FOR PIEZOELECTRIC MEMS SPEAKERS MODELING

Chiara Gazzola, Valentina Zega, Alberto Corigliano, Pierrick Lotton, Manuel  
Melon

► **To cite this version:**

Chiara Gazzola, Valentina Zega, Alberto Corigliano, Pierrick Lotton, Manuel Melon. LUMPED-PARAMETERS EQUIVALENT CIRCUIT FOR PIEZOELECTRIC MEMS SPEAKERS MODELING. 10th Convention of the European Acoustics Association (Forum Acusticum 2023), Sep 2023, Turin, Italy. hal-04266242

**HAL Id: hal-04266242**

**<https://univ-lemans.hal.science/hal-04266242v1>**

Submitted on 31 Oct 2023

**HAL** is a multi-disciplinary open access archive for the deposit and dissemination of scientific research documents, whether they are published or not. The documents may come from teaching and research institutions in France or abroad, or from public or private research centers.

L'archive ouverte pluridisciplinaire **HAL**, est destinée au dépôt et à la diffusion de documents scientifiques de niveau recherche, publiés ou non, émanant des établissements d'enseignement et de recherche français ou étrangers, des laboratoires publics ou privés.



Distributed under a Creative Commons Attribution 4.0 International License

# LUMPED-PARAMETERS EQUIVALENT CIRCUIT FOR PIEZOELECTRIC MEMS SPEAKERS MODELING

Chiara Gazzola<sup>1\*</sup>      Valentina Zega<sup>1</sup>      Alberto Corigliano<sup>1</sup>  
Pierrick Lotton<sup>2</sup>      Manuel Melon<sup>2</sup>

<sup>1</sup> Department of Civil and Environmental Engineering, Politecnico di Milano, Italy

<sup>2</sup> Laboratoire d'Acoustique de l'Université du Mans (LAUM), UMR 6613,  
Institut d'Acoustique - Graduate School (IA-GS), CNRS, Le Mans Université, France

## ABSTRACT

Piezoelectric MEMS speakers are emerging as very promising implementations of loudspeakers at the microscale, as they are able to meet the ever-increasing requirements for modern audio devices to become smaller, lighter and more power efficient [1,2]. However, research work is still needed to accurately capture their mechanical and acoustical response [3]. In this work, we propose a lumped-parameters equivalent circuit for a fast and accurate modeling of this type of devices. The electro-mechanical parameters are derived from a FEM eigenfrequency analysis, for a precise computation of these quantities for arbitrarily complex geometries and an accurate estimation of the shift of the speaker resonance frequency due to an initial non null pre-deflected configuration. The acoustical parameters are instead derived through analytical formulas. Special attention is paid to the air-gaps modeling, by taking into account the acoustic short-circuit between the speaker front and rear sides. The very good matching in terms of Sound Pressure Level among the equivalent circuit predictions, FEM simulations and experimental data demonstrates the ability of the proposed method to accurately simulate the speaker performances, thus representing a fast tool for the design of this class of MEMS speakers.

**Keywords:** Piezoelectric, MEMS, Microspeaker,

\*Corresponding author: chiara.gazzola@polimi.it.

**Copyright:** ©2023 Gazzola et al. This is an open-access article distributed under the terms of the Creative Commons Attribution 3.0 Unported License, which permits unrestricted use, distribution, and reproduction in any medium, provided the original author and source are credited.

Lumped Element Method, IEC 60318-4 coupler

## 1. INTRODUCTION

MEMS speakers have been attracting increasing interest in the last years, as they promise lower power consumption, smaller dimensions and cheaper mass production with respect to traditional micro-speakers [2]. The piezoelectric actuation principle, thanks to the relatively large driving force achievable at low voltages, represents the most promising implementation of loudspeakers at the microscale [1]. Despite a significant number of new structures have been proposed in the recent years [4], MEMS loudspeaker struggle to be competitive in terms of performances compared the non-MEMS counterpart for free field applications. Whereas, some piezoelectric MEMS speaker for in-ear applications have been demonstrated to comply with the market requirements [5]. For this configuration in fact, the pressure chamber effect due to the closed volume defined by the ear canal allows the generation of high SPL without excessive deflections of the mechanical diaphragm.

In 2018, Stoppel et al. [5] firstly proposed the *Mechanically-Open and Acoustically-Closed* (MOAC) design principle as a promising solution for high-performance MEMS speakers. The *mechanically-open* feature comes from the presence of narrow air-gaps between the different mechanical components of the speaker properly sized to allow larger deflections with respect to a closed membrane design. The *acoustically-closed* feature comes instead from the viscous boundary layers induced by the air-gaps that prevent the acoustic short-circuit between the front and rear sides of the speaker. Since then,

different structures with an arbitrarily complex path of air-gaps have been proposed [6, 7].

Lumped element modeling (LEM) and finite element analysis (FEA) can be used to predict the response of MEMS speakers and optimize the design. 3D fully-coupled FEM simulations are however computationally demanding, due to the intrinsic multiphysics nature of the problem and to the high number of degrees of freedom, required by a correct simulation of the different mechanical layers composing the MEMS device, whose thicknesses can differ of more than one order of magnitude. In the design phase, it is thus preferable to use LEM models as simple and efficient tools to predict the response of these devices.

In LEM approach, the representation of spatially distributed physical systems is simplified by using a set of lumped elements when the length scale of the device is much smaller than the wavelength of the governing physical phenomenon. Since the acoustic wavelengths (17.1 m–17.1 mm for 20 Hz–20 kHz) for MEMS speakers are much greater than their sizes (1–10 mm) in almost the whole audible range, LEM is applicable.

An analytical estimation of the electro-mechanical parameters is however not straightforward, since the mechanical structures are often composed by complex geometries. In this work, we propose a lumped-parameters equivalent circuit which relies on an hybrid approach. A FEM prestressed eigenfrequency analysis is exploited for the derivation of the electro-mechanical parameters whereas acoustical parameters are computed through analytical formulas. Moreover, special attention is paid to the air-gaps modeling, by taking into account the acoustic short-circuit between the speaker front and rear sides. The equivalent circuit predictions are compared with full-order FEM simulations and with experimental results, performed on the piezoelectric MEMS speaker recently proposed in [6].

## 2. LUMPED ELEMENT MODEL (LEM)

The equivalent circuit able to simulate the electro-mechano-acoustic response of piezoelectric MEMS speakers in in-ear conditions is reported in Fig. 1. Two transformers model the electro-mechanic and the mechano-acoustic transduction. In the mechanical domain, the vibrating structure is modeled as a one-degree-of-freedom mass-spring-damper system, where  $R_m$ ,  $C_m$  and  $M_m$  represent the participating resistance, mass and compliance of the moving diaphragm, respectively. The

electrical domain is represented by a capacitance  $C_p$ , dielectric and leakage losses are here neglected. The acoustical domain includes a resistor  $R_s$ , representing the viscous losses due to the presence of air-gaps, in a parallel configuration with the capacitor  $C_{bc}$ , representing the back chamber compliance, and the equivalent network of the IEC 60318-4 [8] ear simulator. The output pressure is evaluated in correspondence of the capacitor  $C_5$  of the coupler equivalent network reported in Fig. 2.

The partial acoustic short-circuit at low frequencies is induced by the presence of air-gaps, which put in connection the pressure fields in opposition of phase, generated by the front and rear sides of the speaker. The value of  $R_s$  affects the value of the net volume velocity  $Q - Q_s$  which contribute to the output pressure. In the case of very narrow slits, and as a consequence of very high  $R_s$ ,  $Q_s$  tends to zero. This means that the front volume and the back chamber of the speaker become acoustically decoupled and the acoustic short circuit is completely avoided. Due to technological limitations, the air-gaps width is usually around 10  $\mu\text{m}$ . This width is not sufficiently small to completely circumvent the acoustic short circuit, as already demonstrated in [9]. For a correct evaluation of the speaker response it is thus fundamental to include this phenomenon in the equivalent circuit.

### 2.1 Electro-mechanical lumped-elements

The piezoelectric transduction coefficient  $\alpha$ , the participating mass  $M_m$  and the compliance  $C_m$  are extracted from a FEM prestressed modal analysis implemented in COMSOL Multiphysics® v6.1. The modal analysis assumes the speaker pre-deflected shape caused by fabrication process induced pre-stresses and by the applied Direct Current (DC) voltage as reference configuration.

The expression of the three parameters is derived by imposing the weak formulation of motion considering the piezoelectric constitutive law and then by projecting the equation of motion on the mode of interest.

In the framework of the mathematical description of the linear piezoelectricity, the electro-mechanical coupled constitutive model in the so called *stress-charge* form can be expressed in the following way [10]:

$$\mathbf{T} = \mathbf{C} : \mathbf{S} - \mathbf{e}^T \cdot \mathbf{E} = \mathbf{C} : \mathbf{S} + \mathbf{e}^T \cdot \nabla \phi \quad \text{in } \Omega_p \quad (1)$$

$$\mathbf{D} = \mathbf{e} : \mathbf{S} + \epsilon \cdot \mathbf{E} = \mathbf{e} : \mathbf{S} - \epsilon \cdot \nabla \phi \quad \text{in } \Omega_p \quad (2)$$

where  $\mathbf{T}$  is the second-order stress tensor,  $\mathbf{S}$  is the second-order strain tensor and  $\mathbf{C}$  is the fourth-order elastic stiff-

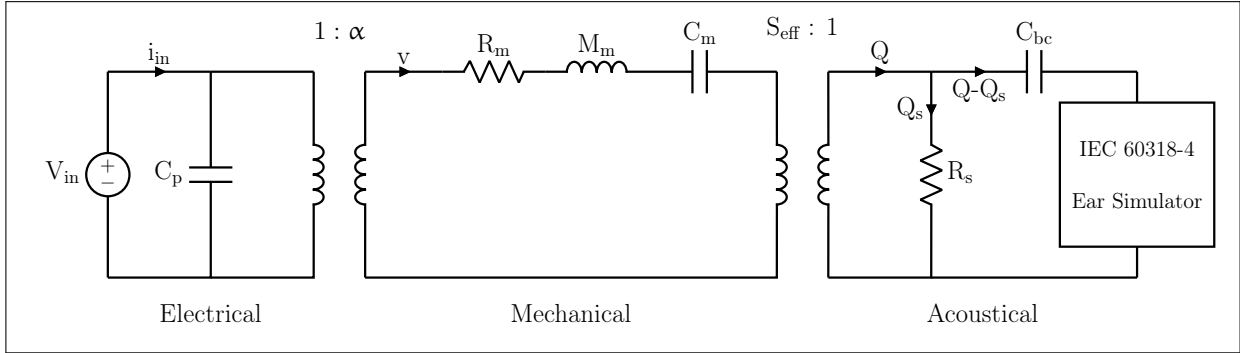


**Figure 1.** Lumped-parameters equivalent circuit able to simulate the electro-mechano-acoustic response of piezoelectric MEMS speakers for in-ear conditions.

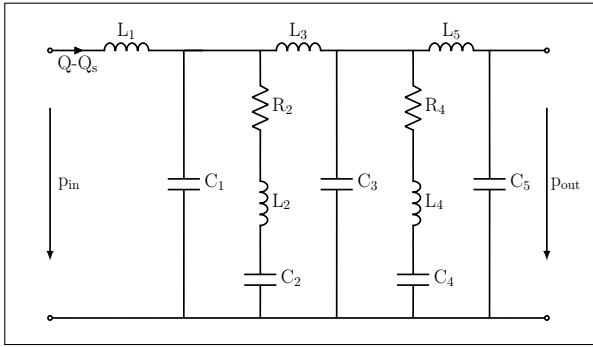


**Figure 2.** Equivalent network of the IEC 60318-4 ear simulator.

ness tensor at constant  $\mathbf{E}$ .  $\mathbf{D}$  is the electric displacement,  $\epsilon$  is the second-order dielectric permittivity tensor at constant  $\mathbf{S}$  and  $\mathbf{e}$  is the third-order piezoelectric coupling tensor. Lastly,  $\mathbf{E}$  is the electric field and  $\nabla\phi$  is the voltage difference.

For the case of thin piezoelectric layer and high electric field (of the order of  $10^7$  V/m, for actuating voltages in the range 0–30 V) it is possible to consider the piezoelectric constitutive law in the one-way formulation [11]. This means that the effect of electrostatics on solid mechanics is considered, but not the vice versa. The constitutive equations then reduce to:

$$\mathbf{T} = \mathbf{C} : \mathbf{S} - \mathbf{e}^T \cdot \mathbf{E} = \mathbf{C} : \mathbf{S} + \mathbf{e}^T \cdot \nabla\phi \quad \text{in } \Omega_p \quad (3)$$

$$\mathbf{D} = \epsilon \cdot \mathbf{E} = -\epsilon \cdot \nabla\phi \quad \text{in } \Omega_p. \quad (4)$$

The restricted weak formulation of the equations of motion can then be formalized by exploiting the principle of virtual work in material form:

$$\int_{\Omega} \rho \ddot{\mathbf{u}} \cdot \tilde{\mathbf{u}} \, d\Omega + \int_{\Omega} \mathbf{T} : \mathbf{S}[\tilde{\mathbf{u}}] \, d\Omega = 0 \quad \forall \tilde{\mathbf{u}} \in C_u(0), \quad (5)$$

where  $\rho$  is the density,  $\mathbf{u}$  is the displacement field,  $\ddot{\mathbf{u}}$  is the time derivative operator applied twice,  $\tilde{\mathbf{u}}$  is a suitable test function belonging to the space  $C_u(0)$ , that is the space of functions that vanish on the boundary where Dirichlet boundary conditions are prescribed.

By inserting the constitutive law in Eqn. (5) and by putting to the right-hand-side the known quantities, the following expression is obtained:

$$\begin{aligned} & \int_{\Omega} \rho \ddot{\mathbf{u}} \cdot \tilde{\mathbf{u}} \, d\Omega + \int_{\Omega} \mathbf{S}[\tilde{\mathbf{u}}] : \mathbf{C} : \mathbf{S}[\mathbf{u}] \, d\Omega \\ & = \int_{\Omega_p} \mathbf{S}[\tilde{\mathbf{u}}] : (\mathbf{e}^T \cdot \mathbf{E}) \, d\Omega \quad \forall \tilde{\mathbf{u}} \in C_u(0), \end{aligned} \quad (6)$$

where  $\Omega_p$  represents the piezoelectric domain. Under the hypothesis of piezoelectric thin film, the electric field generated upon the application of a voltage difference across its thickness  $t_p$  can be expressed as  $\mathbf{E} = E\mathbf{e}_3 = (V_{in}/t_p)\mathbf{e}_3$ , where  $\mathbf{e}_3$  represents the versor of the out-of-plane  $z$  axis. Hence, the right-hand-side of Eqn. (6) reduces to:

$$E \int_{\Omega_p} (S_{11}[\tilde{\mathbf{u}}]e_{31} + S_{22}[\tilde{\mathbf{u}}]e_{32} + S_{33}[\tilde{\mathbf{u}}]e_{33}) \, d\Omega. \quad (7)$$

The reduced order model is obtained by choosing as test function  $\tilde{\mathbf{u}}$  the mechanical eigenmode of interest  $\Phi$ ,

adimensionalized with unit maximum displacement, such as:

$$\tilde{\mathbf{u}}(\mathbf{x}) = \Phi(\mathbf{x}) \quad (8)$$

$$\mathbf{u}(\mathbf{x}) = \Phi(\mathbf{x})q(t) \quad (9)$$

$$\dot{\mathbf{u}}(\mathbf{x}) = \Phi(\mathbf{x})\dot{q}(t) \quad (10)$$

$$\ddot{\mathbf{u}}(\mathbf{x}) = \Phi(\mathbf{x})\ddot{q}(t), \quad (11)$$

where  $q(t)$  represents the modal coordinate. Inserting the abovementioned equations into Eqn. (6) means projecting the equations of motion on the mode under consideration. The corresponding one-degree-of-freedom equation reads:

$$\begin{aligned} \ddot{q}(t) \int_{\Omega} \Phi^T \rho \Phi \, d\Omega + q(t) \int_{\Omega} \mathbf{S}[\Phi] : \mathbf{C} : \mathbf{S}[\Phi] \, d\Omega \\ = E \int_{\Omega_p} (S_{11}[\Phi]e_{31} + S_{22}[\Phi]e_{32} + S_{33}[\Phi]e_{33}) \, d\Omega, \end{aligned} \quad (12)$$

where the modal mass, the modal compliance and the piezoelectric transduction factor can be identified:

$$M_m \ddot{q}(t) + \frac{1}{C_m} q(t) = F_{in} = E\gamma = \frac{V}{t_p} \gamma = V_{in} \alpha. \quad (13)$$

Assuming an harmonic excitation and recasting the equation of motion in terms of velocity, Eqn. (13) becomes:

$$j\omega M_m \dot{q} + \frac{1}{j\omega C_m} \dot{q} = V_{in} \alpha. \quad (14)$$

The current  $v$  which flows in the mechanical domain of the circuit represents the maximum speaker velocity, *i.e.* the velocity corresponding to the point at which the  $\Phi$  component is equal to 1. Having the maximum velocity, the velocity profile in the whole speaker domain can be reconstructed through Eqn. (10).

From the definition of the volume velocity, it is possible to derive the expression of the effective area  $S_{eff}$  used to couple the mechanical domain and the acoustical domain:

$$Q = \int_{\Omega} \dot{u} \, d\Omega = v \int_{\Omega} \Phi \, d\Omega = v S_{eff}. \quad (15)$$

The last parameter to be determined in the electro-mechanical domain is the piezoelectric capacitance  $C_p$ . The latter can be computed by considering the standard formula for parallel plate capacitors [10]:

$$C_p = \frac{\epsilon_r \epsilon_0 A_p}{t_p}, \quad (16)$$

where  $\epsilon_r$  is the relative permittivity of the dielectric material,  $\epsilon_0$  the vacuum permittivity and  $A_p$  the piezoelectric area.

## 2.2 Acoustic lumped-elements

The acoustical lumped-elements are derived through analytical formulas.

The main effect of the back chamber is a stiffening of the speaker, represented in the equivalent circuit through the compliance  $C_{bc}$ . The latter can be evaluated as [12]:

$$C_{bc} = \frac{V_{bc}}{\rho_0 c_0^2}, \quad (17)$$

where  $V_{bc}$  is the back chamber volume,  $\rho_0$  is the air density and  $c_0$  is the speed of sound in air.

The lumped-element  $R_s$  introduced in the speaker equivalent circuit represents the losses which occur inside the slits due to the air viscosity. The resistance value for a single rectangular slit can be deduced by considering the reduced Navier-Stokes equation for a Poiseuille flow [13] and reads:

$$R_s = \frac{12\mu t_{pl}}{l_s w_s^3}, \quad (18)$$

where  $t_{pl}$  is the out-of-plane thickness of the speaker,  $l_s$  is the length of the slit and  $w_s$  its width.

The speaker geometry is usually characterized by a set of multiple air-gaps [6,7]. Considering  $n$  slits, the total resistance reads:

$$R_s = \frac{1}{\frac{1}{R_1} + \dots + \frac{1}{R_n}}, \quad (19)$$

being the different air-gaps in a parallel configuration.

## 3. REFERENCE SPEAKER

The piezoelectric MEMS speaker taken as reference to validate the equivalent circuit prediction is the one recently proposed in [6]. The schematic view of the speaker is shown in Fig. 3a. The moving mechanical structure consists of four trapezoidal actuators (orange in Fig. 3) connected to a central squared piston (green in Fig. 3) through a set of properly sized folded elastic springs (yellow in Fig. 3). The different mechanical components are separated by 10  $\mu\text{m}$ -width air-gaps (black in Fig. 3).



The four trapezoidal actuators are fixed to the substrate through an external silicon frame (gray in Fig. 3). The total footprint of the device is  $4.5 \times 4.5 \text{ mm}^2$ , comprising the  $350 \mu\text{m}$  width of the external frame. The linear electro-mechanical vibration mode occurs at  $10.9 \text{ kHz}$  and its modal shape function is depicted in Fig. 3b. The electro-mechanical lumped parameters of the speaker under investigation are reported in Tab. 1.

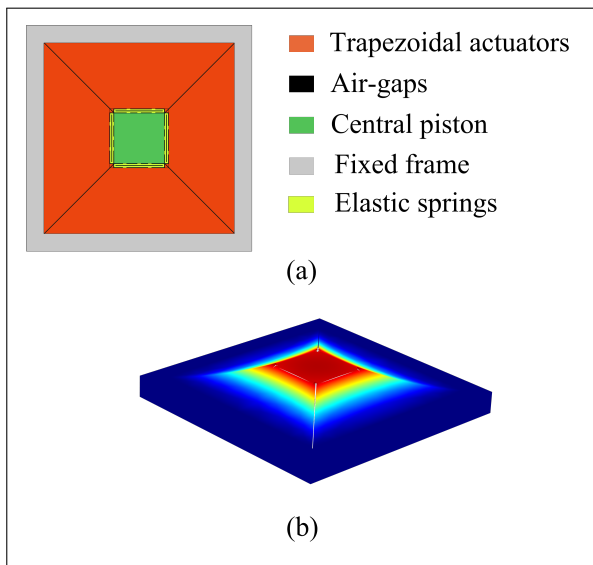


**Figure 3.** (a) Schematic view of the reference piezoelectric MEMS speaker [6] and (b) electro-mechanical modal shape function of its first resonant mode with contour of the displacement field shown in color.

**Table 1.** Parameters of the electro-mechanical lumped-elements.

Parameter	Value	Unit
$C_p$	68	nF
$\alpha$	$5.87 \cdot 10^{-4}$	N/V
$C_m$	$2.25 \cdot 10^{-3}$	m/N
$M_m$	$9.85 \cdot 10^{-8}$	kg
$S_{\text{eff}}$	$3.93 \cdot 10^{-6}$	$\text{m}^2$

#### 4. LEM VERSUS FEM RESULTS

The equivalent circuit predictions in terms of SPL for an actuation voltage of  $12 \text{ V}$  of bias plus  $5 \text{ V}_{\text{pp}}$  are reported in Fig. 4 with blue solid line. The used lumped-parameters of the coupler equivalent circuit are listed in Tab. 2. It is worth to note that the equivalent circuit presented in Fig. 2 has been slightly modified in order to match the transfer function of the coupler implemented in COMSOL Multiphysics® [14] used in the FEM model. In particular, to damp the half-wavelength resonance of the coupler, three resistors  $R_1$ ,  $R_3$  and  $R_5$  were added to the branch of  $C_1$ ,  $C_3$  and  $C_5$ , respectively.

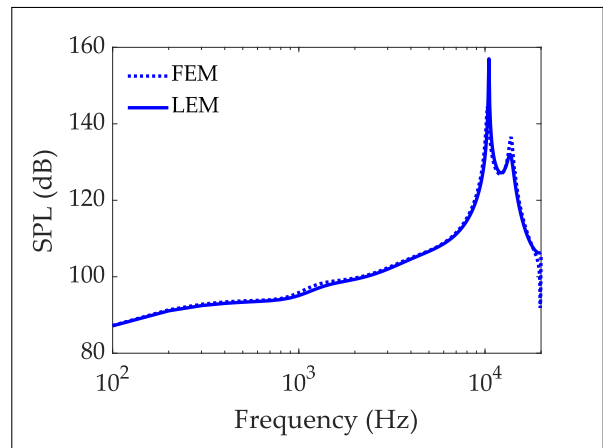


**Figure 4.** Comparison between SPL predictions of the equivalent circuit (solid blue line) and of the FEM model (dashed blue line) for a bias voltage of  $12 \text{ V}$  plus an alternating voltage of  $5 \text{ V}_{\text{pp}}$ .

The LEM SPL prediction is compared with the one of an electro-mechano-acoustic Finite Element model implemented in COMSOL Multiphysics®, that takes into account (i) the elasto-dynamic behaviour of the mechanical structure, (ii) the electro-mechanical coupling through the piezoelectric constitutive law, (iii) the mechano-acoustic coupling between the mechanical structure and the acoustic domains on the front and rear sides of the speaker, (iv) the boundary layer induced by the viscous properties of the air in the narrow gaps, and (v) the in-ear condition through the coupler model available in COMSOL Multiphysics® [14]. The SPL curve derived with the FEM model is depicted in Fig. 4 with a blue dashed line. An excellent agreement in the whole frequency range is demonstrated.

**Table 2.** Parameters of the modified equivalent circuit of the IEC 60318-4 ear occluded simulator.

Parameter	Value	Unit
$L_1$	82.9	$\text{Pa s}^2 \text{m}^{-3}$
$L_2$	9400	$\text{Pa s}^2 \text{m}^{-3}$
$L_3$	130.3	$\text{Pa s}^2 \text{m}^{-3}$
$L_4$	983.8	$\text{Pa s}^2 \text{m}^{-3}$
$L_5$	133.4	$\text{Pa s}^2 \text{m}^{-3}$
$C_1$	$0.7 \cdot 10^{-12}$	$\text{Pa m}^{-3}$
$C_2$	$2.34 \cdot 10^{-12}$	$\text{Pa m}^{-3}$
$C_3$	$1.5 \cdot 10^{-12}$	$\text{Pa m}^{-3}$
$C_4$	$2.73 \cdot 10^{-12}$	$\text{Pa m}^{-3}$
$C_5$	$1.517 \cdot 10^{-12}$	$\text{Pa m}^{-3}$
$R_1$	$4.22 \cdot 10^5$	$\text{Pa s m}^{-3}$
$R_2$	$55.66 \cdot 10^6$	$\text{Pa s m}^{-3}$
$R_3$	$4.22 \cdot 10^5$	$\text{Pa s m}^{-3}$
$R_4$	$27.99 \cdot 10^6$	$\text{Pa s m}^{-3}$
$R_5$	$4.22 \cdot 10^5$	$\text{Pa s m}^{-3}$

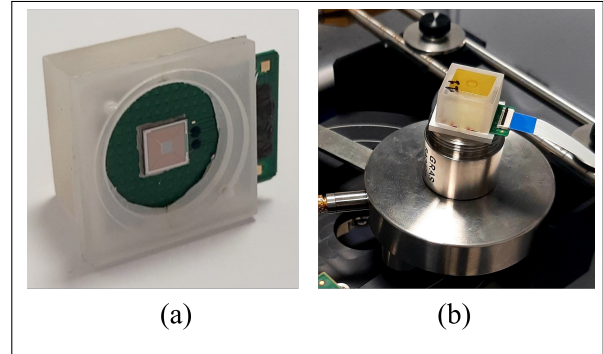


**Figure 5.** (a) Picture of the fabricated piezoelectric MEMS speaker mounted on a custom PCB and coupled with the package for in-ear acoustic tests. (b) Picture of the Device Under Test (DUT) mounted on the ear simulator G.R.A.S. RA0402.

## 5. LEM VERSUS EXPERIMENTAL RESULTS

The SPL evaluated through the proposed equivalent circuit is also compared with experimental measurements carried out on prototypes of the speaker presented in [6], produced by STMicroelectronics. For experimental tests, the device was mounted on a custom Printed Circuit Board (PCB) and coupled with an ABS (Acrylonitrile Butadiene Styrene) thermoplastic package composed by a back chamber of  $1 \text{ cm}^3$  and a front adapter of height of 1 mm to connect the speaker with the ear simulator (Fig. 5). The experimental set-up includes the anechoic chamber G.R.A.S. AL0030-S2, the ear simulator G.R.A.S. RA0402 together with the microphone G.R.A.S. 46 BD  $\frac{1}{4}$ ". The Audio Analyzer (APx525) allows to generate DC and AC signals for the MEMS actuation and to convert the signal from the microphone into SPL data. The SPL curve measured for a DC voltage of 12 V and an AC voltage of  $5 V_{pp}$  is reported in Fig. 6 with a red dashed line. For the comparison with experimental results, the value of  $R_m$  has been tuned by considering a mechanical  $Q_m$  factor of 10, based on typical values used for this type of structures. Moreover, the damping of the coupler has been further augmented, by increasing  $R_1$ ,  $R_3$  and  $R_5$  of a factor of 1.5, since the transfer function of the numer-

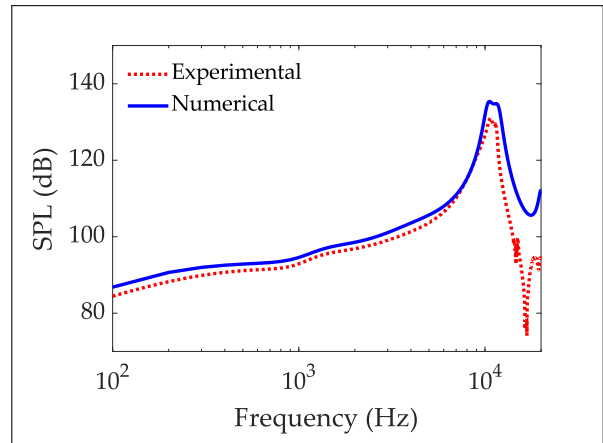


**Figure 6.** Comparison between numerical (blue curve) and experimental (red curve) SPL frequency spectra evaluated in the ear simulator for a bias voltage of 12 V plus an alternating voltage  $5 V_{pp}$ .

ical coupler above 10 kHz is different from the one of the coupler used in the experiments [15].

The agreement between the two curves is very good below 10 kHz, range in which the ear simulator is able to accurately reproduce the acoustical behaviour of the ear canal [16]. The discrepancies in the speaker resonance region is due to the lack of knowledge of the real mechanical  $Q_m$  factor, that can be hardly estimated from this curve with standard formulas being too close to the coupler resonance.

## 6. CONCLUSION

A lumped-parameters equivalent circuit for a fast and accurate modeling of piezoelectric MEMS speaker has been proposed. The derivation of the electro-mechanical parameters from a FEM eigenfrequency analysis allows for a precise computation of these quantities for arbitrarily complex geometries and to consider the shift in the speaker resonance frequency due to an initial non null pre-deflected configuration. The proposed equivalent circuit takes also into account the acoustic short-circuit between the speaker front and rear sides, induced by the presence of air-gaps which separate the different mechanical components of the speaker. The very good matching in terms of SPL among the equivalent circuit predictions, FEM simulations and experimental data demonstrates the ability of the proposed method to accurately simulate the speaker performance, thus representing a fast tool for the design of this class of MEMS speakers.

## 7. ACKNOWLEDGMENTS

The authors would like to thank STMicroelectronics for the production of the prototypes and in particular Fabrizio Cerini and Silvia Adorno for the precious contribution in the experimental tests.

## 8. REFERENCES

- [1] H. Wang, Y. Ma, Q. Zheng, K. Cao, Y. Lu, and H. Xie, "Review of recent development of MEMS speakers," *Micromachines*, vol. 12, no. 10, p. 1257, 2021.
- [2] A. Rusconi, S. Costantini, and C. Prelini, "Micro Speakers," in *Silicon Sensors and Actuators*, pp. 651–676, Springer, 2022.
- [3] H.-H. Cheng, S.-C. Lo, Z.-R. Huang, Y.-J. Wang, M. Wu, and W. Fang, "On the design of piezoelectric mems microspeaker for the sound pressure level enhancement," *Sensors and Actuators A: Physical*, vol. 306, p. 111960, 2020.
- [4] R. Liechti, S. Durand, T. Hilt, F. Casset, C. Dieppedale, and M. Colin, "High performance piezoelectric mems loudspeaker based on an innovative wafer bonding process," *Sensors and Actuators A: Physical*, vol. 358, p. 114413, 2023.
- [5] F. Stoppel, A. Männchen, F. Niekiet, D. Beer, T. Giese, and B. Wagner, "New integrated full-range mems speaker for in-ear applications," in *2018 IEEE Micro Electro Mechanical Systems (MEMS)*, pp. 1068–1071, IEEE, 2018.
- [6] C. Gazzola, V. Zega, F. Cerini, S. Adorno, and A. Corigliano, "On the design and modeling of a full-range piezoelectric MEMS loudspeaker for in-ear applications." under review.
- [7] T.-C. Wei, Z.-S. Hu, S.-W. Chang, and W. Fang, "On the design of piezoelectric mems microspeaker with high fidelity and wide bandwidth," in *2023 IEEE 36th International Conference on Micro Electro Mechanical Systems (MEMS)*, pp. 127–130, IEEE, 2023.
- [8] IEC 60318-4: 2010, "Simulators of human head and ear-part 4: Occluded-ear simulator for the measurement of earphones coupled to the ear by means of ear inserts. standard," *International Electrotechnical Commission*, 2010.
- [9] F. Stoppel, F. Niekiet, T. Giese, S. Gu-Stoppel, A. Männchen, J. Nowak, D. Beer, and B. Wagner, "Novel type of mems loudspeaker featuring membrane-less two-way sound generation," in *Audio Engineering Society Convention 143*, Audio Engineering Society, 2017.
- [10] A. Corigliano, R. Ardito, C. Comi, A. Frangi, A. Ghisi, and S. Mariani, *Mechanics of microsystems*. John Wiley & Sons, 2018.
- [11] A. Frangi, A. Opreni, N. Boni, P. Fedeli, R. Carminati, M. Merli, and G. Mendicino, "Nonlinear response of pzt-actuated resonant micromirrors," *Journal of Microelectromechanical Systems*, vol. 29, no. 6, pp. 1421–1430, 2020.
- [12] J. Merhaut, *Theory of electroacoustics*. McGraw-Hill College, 1981.
- [13] S. D. Senturia, *Microsystem design*. Springer Science & Business Media, 2007.





- [14] COMSOL Multiphysics, *Generic 711 Coupler — An Occluded Ear-Canal Simulator*. accessed on 21 January 2023.
- [15] “GRAS RA0402 Prepolarized High-Frequency Ear Simulator.”
- [16] M. R. Stinson, “Implications of ear canal geometry for various acoustical measurements,” *The Journal of the Acoustical Society of America*, vol. 74, no. S1, pp. S8–S8, 1983.

